

Analysis and Design of Viscoelastic Adhesively Bonded Tubular Joint

Abouel-Kasem, A.*

Mechanical Eng. Dept., Faculty of Eng.-Rabigh, King Abdulaziz University, P.O. Box 344 Rabigh 21911, Kingdom of Saudi Arabia.
aaahmed2@kau.edu.sa

Department of Mechanical Engineering, Assiut University, Assiut 71516, Egypt

Hassab -Allah, I. M.

Mechanical Engineering Department, Assiut University, Assiut 71516, Egypt, hasa57ibm@yahoo.com

Nemat-Alla, M. M.

Mechanical Engineering Department Kafrelsheikh University, Egypt, nematala@acc.aun.edu.eg

Abstract

From the survey of works about the study of viscoelastic adhesively bonded tubular joint, it was found that a little amount of data is available about the effects of viscoelastic properties of adhesive material on the overall performance of adhesively bonded joints. In the current investigation, stress analysis was carried out for six different geometries of adhesively bonded tubular joints under quasi-static internal pressure, taking into consideration the viscoelastic properties of the adhesive material. Lifetime investigation was carried out for the adopted joints under open and closed end conditions, based on the experimental data of the mechanical properties for the viscoelastic adhesive. Finite element method was adopted through the current investigation considering non-linear viscoelastic behavior of the adhesive. The effects of joint geometry and loading conditions on the lifetime and the equivalent stresses were investigated. From the obtained results it was found that double scarf with external sleeve and stepped adhesively bonded joints are the most appropriate joints under open end condition. In addition for closed end condition butt joint with external sleeve and external recessed sleeve joint are the most appropriate joints.

Keywords: Viscoelasticity; Lifetime; FEM; Adhesively bonded tubular joint; Generalized Maxwell model.

Article history: Received 3 Jan 2014, Accepted 30 Jan 2014

1. Introduction

Recently, adhesively bonded tubular structures are extensively used in aircrafts, automobiles, pipelines, etc. Structural performance of adhesively bonded tubular joints with various configurations, such as lap, butt and butt with reinforced sleeve, etc., has been investigated under quasi-static and dynamic loading (e.g., Hassab-Allah, 2002, Jeandrou, 1991, Ahmed, et al., 1989, Khalil, 1994, Vaziri and Hashemi, 2002). For most designs of adhesively bonded joints the principal assumption is the elastic behavior of the adhesive layer (see for example Hassab-Allah, 2002, Apalak and Davies, 1994, Tsai

and Morton, 1994, Mori and Sugibayashi, 1992, Chen and Cheng, 1990, Kyogoku, et al., 1987. In practice, new adhesives such as rubber-modified epoxies have a large plastic strain to failure. Therefore, the elastic-plastic behavior of these types of adhesively bonded joints was investigated by Apalak and Engin, 2002, Ozel and Kadioglu, 2002, Crocombe and Bigwood, 1992. According to Yu, et al., 2001, the elastic and elastic-plastic behaviors of the adhesive is not suitable for many adhesives that have viscoelastic behavior. This maximizes the use of viscoelastic analysis for the adhesively bonded joints, where the re-distribution of stresses and strains that occurs in the joints during the viscoelastic

* Corresponding author

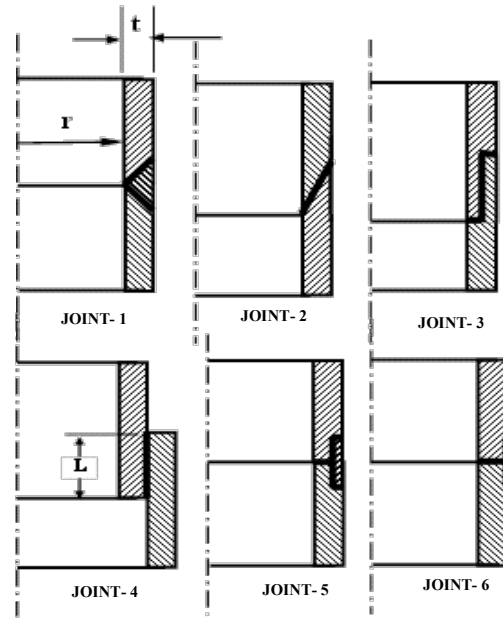
deformation influences the strength of the joints considerably.

From the survey of works (e.g., Apalak, et al., 2003, Nguyen and Kedward, 2001, Fujii, 1993, Miyano, et al., 1982, Heymans, 2003, Feng, et al., 2005) about the study of viscoelastic adhesively bonded tubular joint, it was found that a little amount of data is available about the viscoelastic behavior of the adhesive materials. Therefore the role of viscoelastic properties of adhesive material on the overall performance of adhesively bonded joints needs more investigations. In the present work, stress analysis of adhesively bonded tubular joints with different joint geometries was carried out under quasi-static internal pressure, taking into consideration the viscoelastic behavior of the adhesive material. An approach for the lifetime estimation of the adhesively bonded tubular joint was carried out. Six tubular bonded joints with different geometries, shown in Fig. 1, are adopted through the current investigations. Finite element method was used considering nonlinear viscoelastic adhesive behavior. The effects of joint geometries and loading conditions on the lifetime and the equivalent stress were investigated. The optimum joint geometry was determined based on lifetime and equivalent stresses, for open and closed end conditions.

2. Viscoelastic Lifetime Analysis

The simple linear viscoelastic models can not represent the behavior of adhesives systems well. Therefore, nonlinear viscoelastic material model was adopted throughout the current investigations. Generally the viscoelastic deformation consists of three components: elastic, high elastic and viscous. Different models with discrete set of elastic modulus and relaxation times can successfully represent the viscoelastic behavior of many materials. Generalized Maxwell model, shown in Fig. 2, has great capabilities in representing the nonlinear viscoelastic behaviors. Milašienė, et al., 2003, study and predict stress relaxation in laminated leather in order to provide the possibility to investigate the time dependence shown by different system layers of laminated leather and understanding their viscoelastic behavior. They adopted the generalized Maxwell model which possesses a regular spectrum of relaxation times that successfully describes stress relaxation behavior of the leather in non-linear regions. Abouel-Kasem and Lazarev, 2000, investigated micro viscoelastic model, of rubber, that used in the numerical analysis and design of machine parts. They found that the relaxation and creep

behaviors of the rubber material were successfully represented by the generalized Maxwell model. According to Fujii, 1993, Milašienė, et al., 2003, Abouel-kasem and Lazarev 2000, Sato and Toda, 2004, the generalized Maxwell model was successfully used in representing the viscoelastic behavior of different materials. Therefore, the generalized Maxwell model will be adopted through the current investigations to represent the viscoelastic behavior of the considered adhesive material.



JOINT-1. Double scarf with external sleeve.
JOINT-2. Tubular scarf.
JOINT-3. Stepped joint.
JOINT-4. Tubular over lapped joint.
JOINT-5. External recessed with external sleeve.
JOINT-6. Tubular butt joint with external reinforcing sleeve.

Fig. 1. Considered types of tubular joint

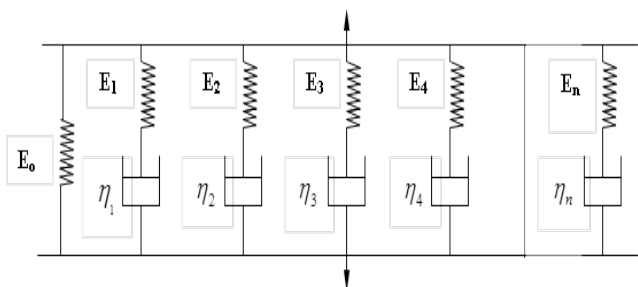


Fig. 2. Generalized Maxwell model

The relaxation modulus for the generalized Maxwell model can be expressed as:

$$E(t) = E_0 + \sum_{k=1}^n E_k e^{-t/\tau_k} \quad (1)$$

where τ_k is the relaxation time of element k, $\tau_k = \frac{\eta_k}{E_k}$, E_0 is the quasi-equilibrium value of the modulus of elasticity, n is the total number of Maxwell elements, E_k is the Young's modulus for element number k and η_k is the coefficient of viscosity of the Maxwell element.

It is well known that the relaxation modulus and creep compliance are connected by a simple relation between their Laplace transforms as;

$$J(S)E(S) = \frac{1}{S^2} \quad (2)$$

Applying Laplace transforms on Eq. (1) and substituting it into Eq. (2), Laplace transforms of the creep compliance for the generalized Maxwell model may be obtained as;

$$J(S) = \frac{1}{E_0 S + \sum_{k=1}^n E_k \frac{S^2 \eta_k}{E_k + S}} \quad (3)$$

Due to the complexity of Laplace transforms of the creep compliance for the generalized Maxwell model, Eq. (3), it is impossible to obtain explicit function for the creep compliance in the time domain. In such case a numerical scheme may be carried out based on the integral form of the inverse Laplace transform to obtain the creep compliance in the time domain.

For compressible or incompressible nonlinear viscoelastic material the stress rate tensor, for the general Maxwell model, can be expressed as:

$$\dot{\sigma}_{ij} = \dot{\sigma}_{ij}^e - \frac{1}{\tau_k} \sigma_{ij} \quad (4)$$

where $\dot{\sigma}_{ij_k}$ is the stress rate tensor of element number k, $\dot{\sigma}_{ij_k}^e$ is the rate of elastic stresses tensor of element number k, σ_{ij_k} is the stress tensor of element number k.

The nonlinear elastic behavior of viscoelastic material is described by potential energy polynomial as:

$$W = \sum_{i,j} C_{ij} (I_1 - 3)^i (I_2 - 3)^j \quad (5)$$

where, I_1 and I_2 are the first and second invariants of the deviatoric strains and C_{ij} are material constants. C_{ij} are constants that can be determined from experimental data generated from both of uniaxial tension and compression tests.

The lifetime estimation of viscoelastic adhesive is an important factor for the design of the adhesively bonded joints. According to Abouel-Kasem, 2006, the lifetime of the viscoelastic material in cases of uniaxial creep tension and plane stress states can be determined by the following equations:

$$\log \tau = \log C + \frac{52.261 U_0}{273 + T_c} - b \log(\boldsymbol{\sigma}) \quad (6)$$

$$\begin{aligned} \log \tau = \log C + & \frac{52.261 [U_0 + a(\boldsymbol{\sigma}_s)^2]}{273 + T_c} \\ & - b \log(1.5 \boldsymbol{\sigma}_{dev_1}) \end{aligned} \quad (7)$$

Where τ is the lifetime, service time to failure, U_0 is the initial activation energy of rupture process, b is the static strength exponent, $\log C$ is the pre-exponential coefficient, a is a constant value; $\boldsymbol{\sigma}_{dev_1}$ is the first principal deviator of stress, $\boldsymbol{\sigma}_s$ is the hydrostatic stresses and T_c is the temperature (°C).

It is possible to calculate lifetime not only on edge of the viscoelastic parts, but also inside by equation (7) after experimental determination of the lifetime parameters. For calculating the lifetimes of the viscoelastic material parts at different temperatures a computer program was written using C++ software and formula 7, the input data of the activation characteristics of elastomer (b , U_0 , $\log C$) and the parameter (a) which are determined experimentally. The program was realized in the version of finite element method FEM. Solution problems of viscoelastic parts were considered as incompressible by Abouel-Kasem, 2006.

3. Adhesive Viscoelastic Properties

The viscoelastic properties of the adhesive material, cold-cure epoxy E27 supplied by Permabond, experimentally obtained by Yu, et al., 2001, were adopted through the current investigations. Where, creep tests were carried out at different applied stresses, 35 MPa, 40 MPa and 45 MPa. Figure 3 shows the variation of the creep compliance, $J(t)$, versus time at different applied stresses. It's clear that the creep compliances, $J(t)$, at different applied stresses have bad agreement in the rupture

stages. This may be attributed to the fact that near the rupture stage tri-axial stresses are induced. Due to such fact the creep compliance, $J(t)$, of long time, small applied stresses, may have more reality in representing the viscoelastic behavior of the materials. Therefore, the experimental date of the creep compliance extracted from the experimental work by Yu, et al., 2001, of long creep time, at applied stress of 35 MPa, are adopted in representing the viscoelastic behavior of cold cure epoxy E27. According to Yu, et al., 2001, complete ranges of the creep tests data for cold cure epoxy E27 were obtained, at different loads, where, the characteristics primary, secondary and tertiary region of the creep can be seen. From the tertiary regions the variation of the rupture time versus stresses for both of tension and compression quasi-static loads were obtained and represented in Fig. 4.

Also, the stress-strain data, shown in Fig. 5 for cold cure epoxy E27 obtained by Yu, et al., 2001, under tensile and compressive loads will be used.

To obtain the suitable number of elements of the generalized Maxwell model and their assigned values, the all experimental data were inserted in FEM (Ansys software). The numerical scheme was carried to obtain optimum number of elements of the generalized Maxwell model and their assigned values as shown in Fig. 6. The numerically obtained creep compliance data for the generalized Maxwell model and their corresponding experimental values were represented in Fig. 3. They were obtained based on percentage errors of 1% or less between the creep data for the experimental and numerically calculated values.

Finally, the activation characteristic parameters (b , U_0 , $\log C$) and parameter (a) of the viscoelastic adhesive material, cold cure epoxy E27, were determined as follows:

The static strength exponent b is determined from the experimental results for two samples tested with two different tensile stresses from Fig. 4. Two lifetimes τ_1 and τ_2 which, corresponding to different tensile stresses σ_1 and σ_2 were recorded before fracture. The static strength exponent b is calculated using the following relation;

$$b = -\frac{\log \tau_1 - \log \tau_2}{\log \sigma_1 - \log \sigma_2} \quad (8)$$

Two lifetimes τ_1 and τ_2 which corresponding to different temperature T_1 and T_2 at constant stress σ at different temperatures were recorded and used to calculate the activation energy of U_0 as follows:

$$U_0 = \frac{2.303 \cdot (\log \tau_1 - \log \tau_2) \cdot R}{\frac{1}{T_1} - \frac{1}{T_2}} \quad (9)$$

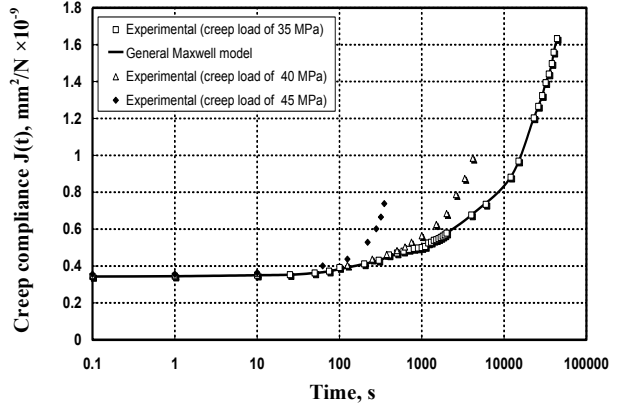


Fig. 3. Variation of creep compliance, $J(t)$, versus time at different applied stresses for cold cure epoxy E27 extracted from Yu, et al., 2001

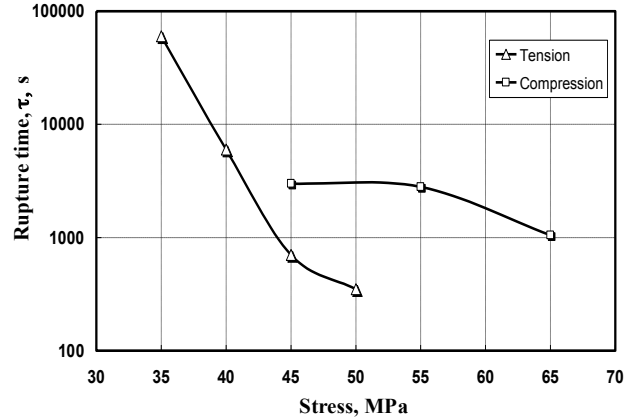


Fig. 4. Rupture time versus stress in case of tension and compression quasi-static loads for cold cure epoxy E27 extracted from Yu, et al., 2001

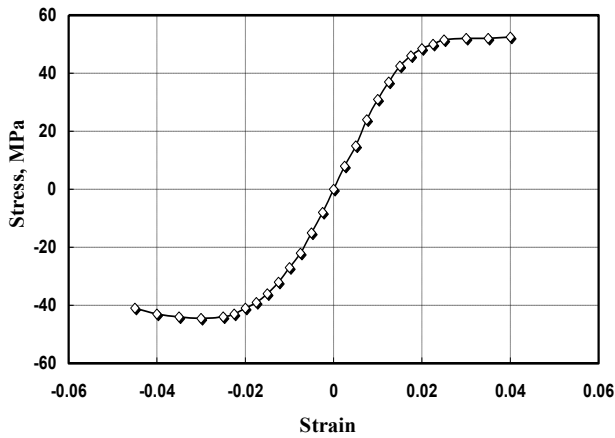


Fig. 5. Stress-strain data for cold cure epoxy E27 obtained by Yu, et al., 2001, under tensile and compressive loads

The parameter $\log C$ is determined from the experimental data point of sample fractures at constant temperature and tension stress. The formula for determining the parameter $\log C$ is

$$\log C = \log \tau - \frac{52.261 \cdot U_0}{273 + T_c} + b \log \sigma \quad (10)$$

The parameter (a) was determined from uniaxial compression test of cylindrical sample between two flat polished chromium-platens. The cylinder/compression platens interface surfaces were lubricated with inert silicone oil. This scheme of lubrication will reduce interface friction coefficient. During the experiment, the cylinder is loaded with a constant load F at temperature $T_c = 20^\circ\text{C}$. The time to the first appearance of fractures is measured. The experimental results for compression cylinder are represented in Fig. 4 (nonlinear part).

At internal points of the cylinder, the hydrostatic pressure is not equal to zero $\sigma_s \neq 0$. To calculate the lifetime at internal points, it is necessary to know the magnitude of the parameter (a). From equation (7), the parameter (a) can be determined as follows:

$$a = \frac{1}{2} \cdot \left[\frac{273 + T_c}{52.261} \left(\log \tau + b \log (1.5 \cdot \sigma_{dev_1}) - \log C \right) - U_0 \right] \quad (11)$$

The first principal deviator stress and hydrostatic pressure of internal point are determined using FEM. From experimental results of time before fracture at the tensile stress $\sigma = 1.5 \cdot \sigma_{dev_1}$ and temperature $T_c = 20^\circ\text{C}$ the parameter (a) can be calculated from equation (11).

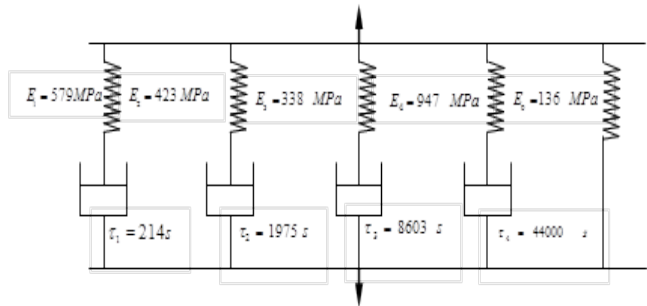


Fig. 6. Generalized Maxwell model that represents cold cure epoxy E27

The activation characteristics of cold cure epoxy E27 (b , U_0 , $\log C$) and the parameter (a) were determined theoretically and experimentally as mentioned above, it was found that cold cure epoxy E27 has the parameters, which are listed in Table 1.

Table 1 Values of activation characteristics (b , U_0 , $\log C$) and parameter (a).

U_0 , kJ/mol	b	$\log C$	$a, \frac{kJ}{mol \cdot (MPa)^2}$
150	18.407	6.6363	9.08×10^{-3}

4. Finite Element Analysis

4.1. Finite Element Mode

Six geometries of adhesively bonded tubular joints were adopted throughout the current investigations, as shown in Fig. 1. Each joint consists of two thick-walled tubes bonded together through an adhesive layer. The tubular joint dimensions are; tube inner radius $r = 20$ mm, tube thickness $t = 6$ mm and different adhesive thickness ta that vary from 0.05 mm to 0.4 mm. In order to obtain the optimum joint, a comparison of lifetime and equivalent stresses for the different joints has been carried out using FEM (STAR for windows by Abouel-kasem and Lazarev, 2000 and 2001). For proper comparison a constant length of adhesive layer, L , of 20 mm was adopted. Each of the considered tubular joints is treated as two-dimensional axisymmetric problem. Due to the geometrical symmetry of joints 1, 5 and 6 about mid plane only one half of the joint have been modeled. While for joints 2, 3 and 4 full joint have been modeled. The tubes and sleeves are assumed to be made of carbon steel that has modulus of elasticity $E = 206$ GPa and Poisson's ratio $\nu = 0.29$.

The initial shapes of the finite element meshes for the considered adhesively bonded tubular joints are shown in Fig. 7. Four-node axisymmetric isoparametric element with four-integration points was used in all models. Two sets of boundary conditions were considered, open and closed ends. For open end condition both of tube ends are axially constrained, zero displacements in the axial direction (z-axis), and an internal pressure is applied at the entire inner surface nodal points in the radial direction (r-axis). While for the closed end condition, one of tube ends was fixed with zero displacement in z-axis and an internal pressure is applied at the entire inner surface nodal points in the radial direction. Due to closed end condition, the upper tube end was subjected to a uniform static pressure p_c :

$$P_c = \frac{pr^2}{t(t+2r)} \quad (12)$$

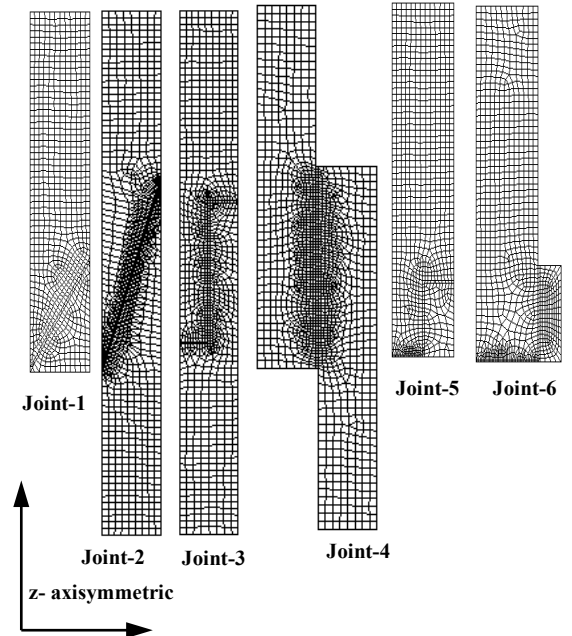
It will be known that the output results of the finite element model are very sensitive for the element size; therefore, it will be necessary to check the effect of element size on the results accuracy. In order to do that, different models with different mesh densities for the different joints should be investigated. From Fig. 1 it is clear that the geometry of the adhesive layer for the considered joints may be classified into two groups. One group has sharp corners, joints 3, 5 and 6. The other group has not sharp corners, joints 1, 2 and 4. Therefore, only one joint of each group may be adopted through the investigation of the effect of the mesh density on the results accuracy, for example joints 1 and 3.

In order to check the effect of mesh density on the results accuracy, different models of different meshes density were used: 1×10 , 2×20 , 3×30 , 4×40 , 5×50 and 6×60 elements, (thickness \times longitudinal number of elements) of the adhesive layer. Finite element simulations for joints 1 and 3 under applied pressure of 25 MPa and 0.4 mm thickness of the adhesive layer under open-end-condition were carried out. The lifetime distribution along the adhesion interface, for joints 1 and 3, was adopted in the investigation of the effect of the mesh density on the results accuracy.

Figure 8 shows a comparison between the lifetime distributions for joint 1 under the adopted meshes densities. It is clear that the large discrepancy in the lifetime distributions appears for 1×10 and 2×20 meshes while the other three different meshes are of satisfactory agreements. This means that the accuracy may have no significant improvement by any more increase of the mesh density beyond 5×50 elements. In order to make a proper comparison the percentage

error in the lifetime distributions, for joint 1, for the meshes 1×10 , 2×20 , 3×30 and 4×40 are compared with respect to the mesh 5×50 . Figure 9 shows a comparison of the percentage error in lifetime along the adhesion interface. It is clear that the minimum percentage error is achieved for the mesh 4×40 compared with the mesh 5×50 . The maximum percentage error for the mesh 4×40 is 2.36%. Therefore the mesh 5×50 is adopted through the current investigations for the joints 1, 2 and 4.

Also, Fig. 10 shows a comparison between the lifetime distributions for joint 3 under the adopted meshes densities. It is clear that large discrepancy in the lifetime distributions appears for 1×10 and 2×20 meshes while the other meshes have satisfactory agreements. It was found that the accuracy has no significant improvement by any more increase of the mesh density beyond 6×60 elements. This may be attributed to the fact that at place of sharp corners or changing geometry, normalized lengths s/L of 0.15 and 0.85, large values of the stress concentrations are induced, where s is the length of the adhesive layer from the internal free edge to the considered point. At such places it is expected that accuracy of the mesh



Joint No.	1	2	3	4	5	6
No. of nodes	2729	5410	3501	4695	2968	3268
No. of elements	864	1743	1108	1512	939	1033

Fig. 7. Finite element meshes of the adopted adhesively bonded tubular joints

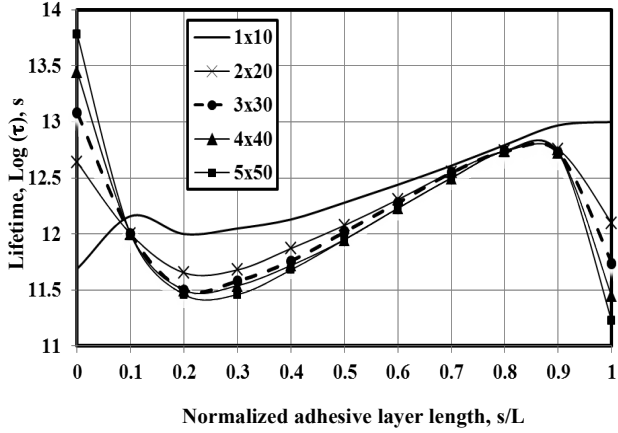


Fig. 8. Lifetime distributions on the adhesion interface for different mesh densities, under applied pressure 25 MPa with 0.4 mm thickness of the adhesive layer, for joint 1 under open end condition

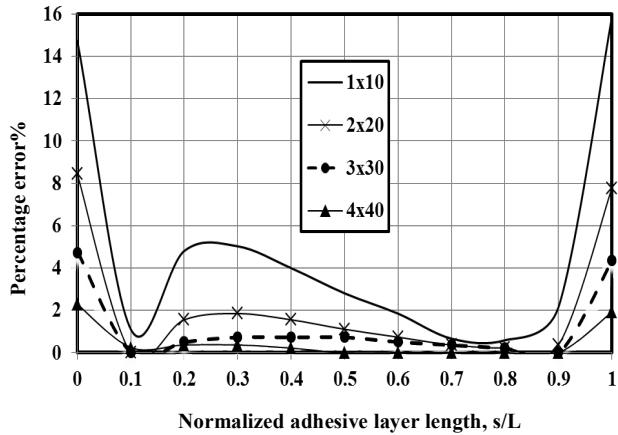


Fig. 9. Comparison of the percentage error of lifetime distributions on the adhesion interface for different mesh densities with respect to the mesh 5×50 for joint 1 under open end condition

density may violate.

In order to make proper comparison, the percentage error in the lifetime distributions for adopted meshes densities with respect to mesh 6×60 are considered and represented in Fig. 11. It is clear that the minimum percentage error is achieved for the mesh 5×50 compared with the mesh 6×60. The maximum percentage error for the mesh 5×50 is 7.5% that occurs at place of sharp corners. Therefore the model of 6×60 elements is adopted through the current investigations for the joints 3, 5 and 6.

Finally, to check the effect of time step length on the results accuracy of the adopted viscoelastic models, different time step lengths of 10, 20, 30, 40, 50, 75 and 100 were used. The obtained results

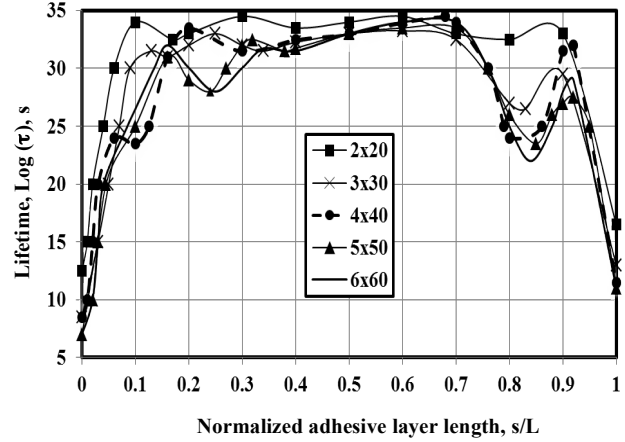


Fig. 10. Lifetime distributions on the adhesion interface for different mesh densities, under applied pressure 25 MPa with 0.4 mm thickness of the adhesive layer, for joint 3 under open end condition

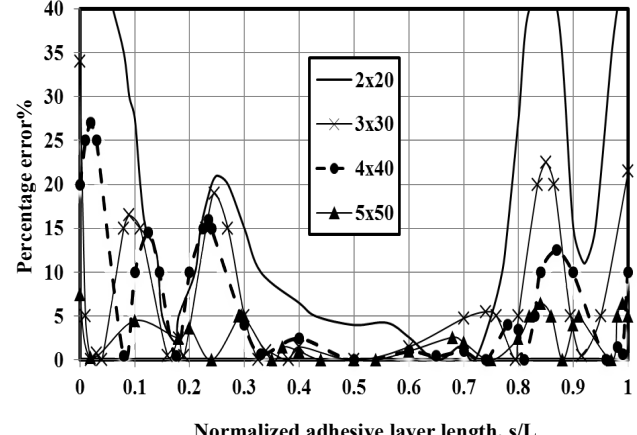


Fig. 11. Comparison of the percentage error of lifetime distributions on the adhesion interface for different mesh densities with respect to the model 6×60 for joint 3 under open end condition

showed that the effects of time step lengths on the results accuracy were of small order and may be neglected. Therefore, the time step increments of 100 were adopted through all the current investigations.

4.2. Strength of Adhesively Bonded Tubular Joint

The mechanical strength of the adhesively bonded tubular joint essentially depends on three parameters:

- adhesion between adhesive and adherends;
- cohesion of the cured adhesive; and
- joint geometry (shape and dimensions)

The modes of failure in the adhesively bonded tubular joints are illustrated in Fig. 12. The surface preparation of the adherends (surface roughness and pre-treatment to remove the oxide films) has great influence on the interfacial failures, for more details see Rider, 1998.

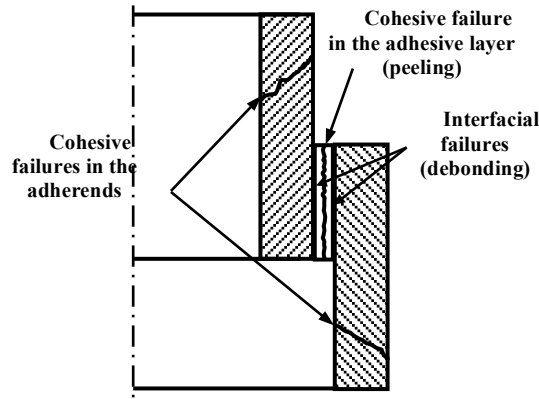


Fig. 12 Different modes of failure in adhesively bonded tubular joints

Interfacial cracks are frequently observed to occur in fabrication and manufacturing processes, such as trapped air bubbles or incomplete wetting between an adhesive and adherends. Wang and Yau, 1981 have shown that the presence of an edge crack in adhesive joints, such as interfacial flaw, can result in a progressive reduction of joint stiffness and the disintegration of the structure, which leads to fracture. The cohesive failures in the adhesive layer, that will be considered here mainly depends on the adhesive properties and the stress distributions through the adhesive layer

The normal stress σ_1 , σ_2 and shear stress τ_{12} components at the adhesive layer especially in the vicinity of the free end are responsible for the crack initiation. The presence of an edge crack in the adhesive layer accompanied with the induced peeling or/and shear stresses will lead to progressive propagation of the crack which reduces the joint stiffness and lead to final fracture. Therefore, the normal and shear stress components in the adhesive layer are of prime importance. During the current investigations equivalent stresses are used instead of normal and shear stress components.

$$\sigma_{eq} = \sqrt{(\sigma_1)^2 + (\sigma_2)^2 + (\tau_{12})^2} \quad (13)$$

The joint shape, adhesive layer thickness and adhesive layer length are the most effective parameters on the strength of the adhesively bonded tubular joints. This is due to their effect on the stress distributions along the bonded joints. Therefore, the main aim of the current investigations is to determine the optimum joint geometry based on minimum equivalent stresses and maximum lifetime.

5. Results And Discussions

The equivalent stresses at internal free edge, as indicated by the arrows shown in Fig. 13, are plotted against elapsed time for applied pressure of 25 MPa under open end condition. The equivalent stresses at internal free edge for the adopted joints obtained from the viscoelastic analysis are represented in Fig. 13. It is clear that the equivalent stress sharply decreases at the beginning of applying pressure. Also, the viscoelastic behavior is clearly induced just after applying the internal pressure. Such case of viscoelastic behavior looks like relaxation case. The high values of the equivalent stresses at zero time represent the nonlinear elastic response only of the viscoelastic material, where there is no viscous response at zero time. This indicates that the severe values of these stresses induced just after applying the internal pressure. If such stress state is accompanied with a free edge crack it will be a dangerous viscoelastic case that may lead to premature failure.

To determine the effect of the applied pressure on the equivalent stresses along the adhesive layer the considered joints were investigated under different pressures. For proper comparison the maximum value of the equivalent stresses along the adhesive layer, for each joint, were adopted. It was found that the maximum values of the equivalent stresses along the adhesive layer have linear variations with the applied pressures, for the considered joints under open and closed end conditions. Therefore, the maximum values of the equivalent stresses were normalized by the applied pressure. Figure 14 shows the variation of the maximum equivalent stress values on the adhesive layer normalized by the applied pressure, at zero time and 1×10^6 seconds, for the considered tubular joints under open end condition. Based on minimum value of the maximum equivalent stresses only it was found that joint 1, double scarf with external sleeve, is the optimum joint. This agrees with the results of Hassab-Allah, 2002.

Figures 15 shows the variation of the maximum values of the equivalent stress along the adhesive layer normalized by the applied pressure, at zero time and 1×10^6 seconds, for the considered tubular joints under closed end condition. Based on minimum value of the maximum equivalent stresses only it was found that Joint-6, butt joint with external sleeve, is the optimum joint.

To justify the previous identifications of the optimum joint, lifetime-investigations were carried out for the adopted (adhesively bonded tubular) joints, using lifetime analysis considered in section 2. Figures 16 and 17 show the variations of the minimum lifetime values on the adhesive layer versus the applied pressure, for 0.4 mm thickness of the adhesive layer under open and closed end conditions respectively.

From Fig. 16 it is clear that joint 1, double scarf with external sleeve, is the optimum joint from the lifetime point of view for open end conditions. This agrees with the results of Hassab-Allah, 2002, and the results obtained from Fig. 14 based on equivalent stress evaluations. This may be attributed to the fact that in case of open end condition, due to the joint

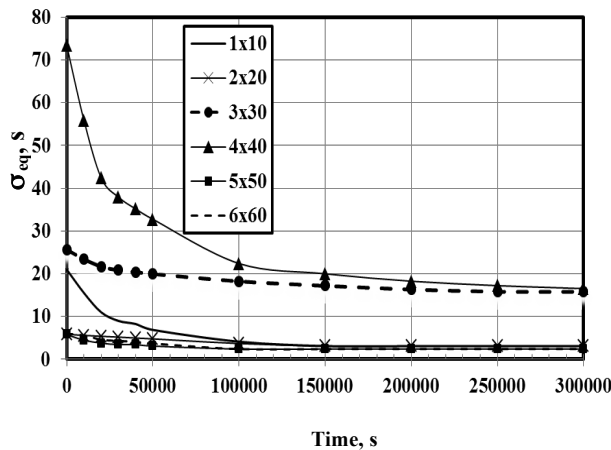


Fig. 13. Variations of the equivalent stresses versus time for the adopted six tubular joints at the internal free edge point (as indicated by arrows) for applied pressure of 25 MPa under open end condition

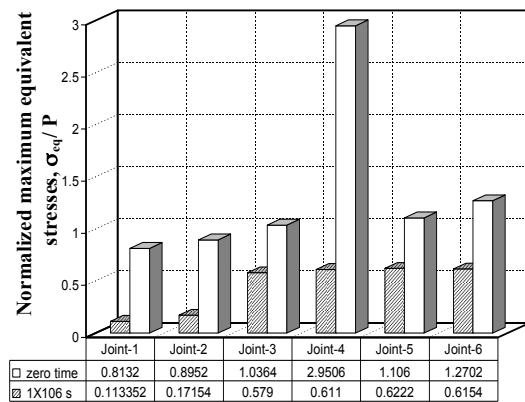


Fig. 14. Variation of the maximum values of the equivalent stress, on the adhesive layer normalized by the applied pressure at zero and 1×10^6 seconds, for the considered tubular joints under open end condition at applied pressure of 25 MPa

geometry, joint 2, 3 and 4 are subjected to peeling while joints 1, 5 and 6 have compressive stresses. In addition, joints 5 and 6 are subjected to direct shear stresses.

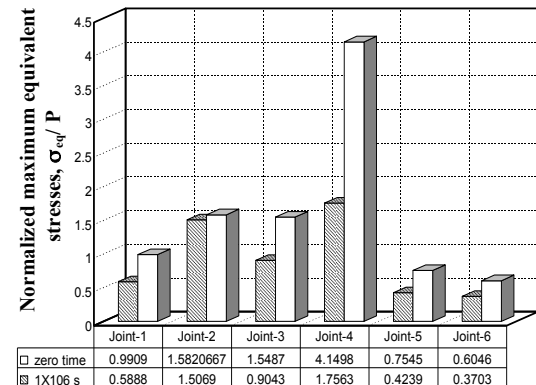


Fig. 15. Variation of the maximum values of the equivalent stress, on the adhesive layer normalized by the applied pressure at zero and 1×10^6 seconds, for the considered tubular joints under closed end condition at applied pressure of 25 MPa

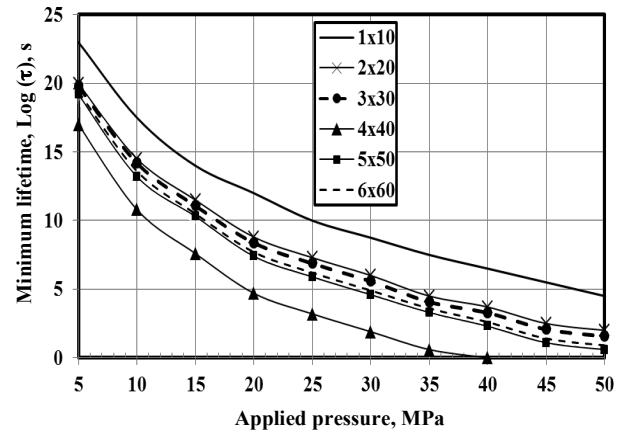


Fig. 16. Variation of the minimum lifetime versus the applied pressure for the considered tubular joints under open end condition

Also, from Fig. 17 it is clear that Joint-6, butt joint with external sleeve, is the optimum joint from the lifetime point of view for closed end conditions. This agrees with the results obtained from Fig. 15 based on equivalent stress evaluations. This is an expected result in case of closed end condition. Where, joints 1, 5 and 6 are subjected to shear stress component. But joint 6 have maximum area that can resist such shear stresses. The agreement of the optimum joint obtained based on equivalent stresses and lifetime evaluations, Figs 14–17, may be attributed to the fact that during lifetime estimation the equivalent, hydrostatic and deviatoric stresses are considered.

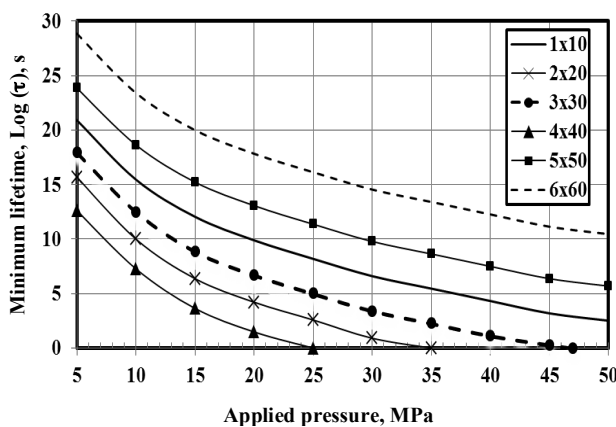


Fig. 17. Variation of the minimum lifetime versus the applied pressure for the considered tubular joints under closed end condition

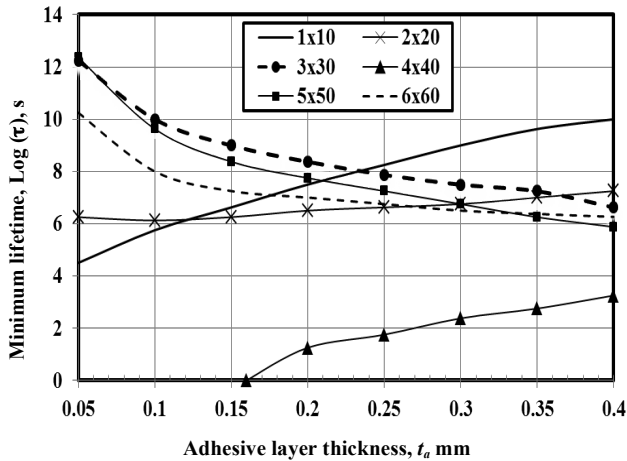


Fig. 18 Variations of the minimum lifetime versus adhesive layer thickness, ta, for the adopted joints at applied pressure of 25 MPa under open end condition

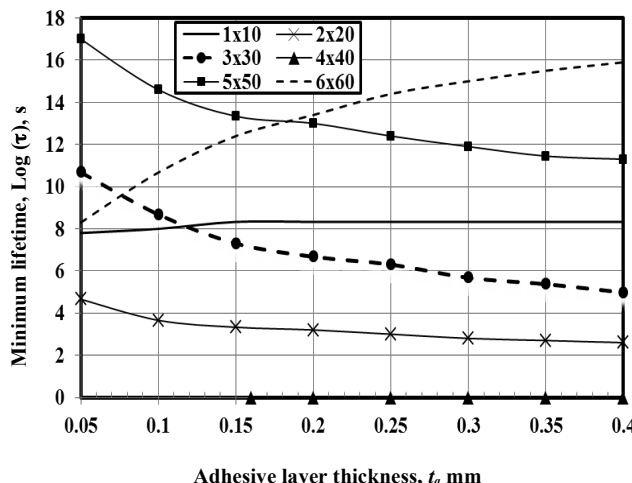


Fig. 19 Variations of the minimum lifetime versus adhesive layer thickness, ta, for the adopted joints at applied pressure of 25 MPa under closed end condition

To investigate the effect of the adhesive layer thickness on the joint lifetime, lifetime of the considered adhesively bonded tubular joints was investigated, for both open and closed end conditions. Different adhesive layer thickness, t_a , that varies from 0.05 to 0.4 mm are considered, while the other parameters of the joints were kept constant. Figures 18 and 19 show the variations of the minimum values of lifetime on the adhesive layer thickness, t_a , at applied pressure of 25 MPa. From Fig. 18 it can be noticed that the joint lifetime, under open end condition, decreases with the increase of the adhesive layer thickness for joints 3, 5 and 6. For joints 1, 2 and 4 lifetime increases with the increase of the adhesive layer thickness. From Fig. 19 it is clear that the joint lifetime, under closed end condition, increases with the increase of the adhesive layer thickness for joint 6. While for joints 2, 3 and 5 lifetime decreases with the increase of the adhesive layer thickness. Also, the lifetime of joint 1 have not reasonable changes with the increase of the adhesive layer thickness. Based on maximum lifetime for open end condition, from Fig. 18, it can be concluded that joint 1 is the optimum joint for adhesive layer thickness greater than 0.23 mm, which is the practical values of the adhesive layer thickness. Where, joint 3 is the optimum joint for adhesive layer thickness less than 0.23 mm. Also for closed end condition, from Fig. 19 it can be concluded that joint 6 is the optimum joint for adhesive layer thickness greater than 0.175 mm, which contains the practical values of the adhesive layer thickness. Where, joint 5 is the optimum joint for adhesive layer thickness less than 0.175 mm. This may be attributed to the fact that loading conditions of the adhesive layer are dependent on the joint geometry. Similar results were obtained for adhesively bonded corner joints by Apalak and Davies 1993.

6. Conclusions

From the current investigations of the viscoelastic adhesively bonded tubular joint, the obtained results may be summarized as follows:

- The viscoelastic behavior of the adhesive material is clearly present just after applying the internal pressure, which increase with the increase of the elapsed time till reach's steady state value. Such case of viscoelastic behavior looks like relaxation.
- The high values of the stresses induced in the adhesive layer at the beginning of load application represent a dangerous case, especially if such stress state is accompanied with edge cracks.

- Based on equivalent stresses and lifetime evaluations, for open end condition, double scarf with external sleeve and stepped adhesively bonded joints are the most appropriate joints.
- For closed end condition butt joint with external sleeve and external recessed sleeve joint are the most appropriate joints.

References

- Abouel-kasem A., Lazarev S.O., 2001. "Calculation of Relaxation and Creep for Designing Sealing of the Oil-Extracting Equipment," XXVIII Week of a Science SPpgTU on Materials of an International Scientific Conference, December 6-11, San Petersburg, Russia, pp. 52-54.
- Abouel-Kasem, A., 2006. "Lifetime Estimation and New design of the Elastomeric Rubber Seals Reinforced with Metal End Caps," Sealing Technology 32, pp.5-9.
- Abouel-kasem, A., Lazarev, S.O., 2000. "Micro Elastoviscoplastic Model of Rubber and Its Usage for Numerical Analysis and Design of Parts," IV th International Conference on Scientific and Technical Problems of Forecasting of Reliability and Durability of Designs and Methods of their solution, November 27-December 2, San Petersburg, Russia, pp. 13-15.
- Ahmed, O. I.; Nassr, A. A., Khalil, A. A., 1989. Design Concepts of Bonded Tubular Lap Joints. Bulletin of the Faculty of Engineering, Assiut University 17, Part 2, pp. 63-68.
- Apalak, M.K., Güne, R and Fidancı, L, 2003. Geometrically Non-Linear Thermal Stress Analysis of an Adhesively Bonded Tubular Single Lap Joint. Finite Elements in Analysis and Design 39, pp. 155-174.
- Apalak, M.K., Davies, R., 1993. Analysis and Design of Adhesively Corner Joints. Int. J. Adhesion and Adhesives 13, pp. 219-235.
- Apalak, M.K., Davies, R., 1994. Aanalysis and Design of Adhesively Corner Joints: Fillet Effect. Int. J. Adhesion and Adhesives 14, pp. 163-174.
- Apalak, M.K., Engin, A., 2002. "Elasto-Plastic Stress Analysis of an Adhesively Bonded Single Lap Joint Subjected to a Bending Moment," 10th Int. Conference on Machine Design and Production, September, Turkey, pp. 291-307.
- Chen, D., Cheng, S., 1990. Stress Distribution in Plane Scarf and Butt Joints. ASME J. of Applied Mechanics 57, pp. 78-83.
- Crocombe, A.D., Bigwood, D.A., 1992. Development of a Full Elasto-Plastic Adhesive Joint Design Analysis. J. of Strain Analysis 27, pp. 211-218.
- Feng, C.-W., Keong, C.-W., Hsueh, Y.-P., Wangc, Y.-Y., Suea, H.-J., 2005. Modeling of Long-Termcreep Behavior of Structural Epoxy Adhesives. Int. J. Adhesion & Adhesives 25, pp. 427-436.
- Fujii, T., 1993. Dynamic Response of Sandwich Beams with an Adhesive Damping Layer (Generalized Maxwell Model for a Viscoelastic Adhesive Layer. Int. J. Adhesion and Adhesives 13, pp.201-209.
- Hassab-Allah, I.M, 2002. Analysis and Design of Adhesively Bonded Tubular Joints under Internal Pressure. Journal of Engineering Science, Assiut University 30, pp. 477-489.
- Heymans, N., 2003. Constitutive Equations for Polymer Viscoelasticity Derived from Hierarchical Models in Cases of Failure of Time-Temperature Superposition. Signal Processing 83, pp. 2345 – 2357.
- Jeandrouau, J.P., 1991. Analysis and Design Data for Adhesively Bonded Joints. Int. J. Adhesion and Adhesives 11, pp. 71-79.
- Khalil, A. A., 1994. "Design and Analysis of Bonded Sleeved Tubular Joints," 1st Int. Conf. on Mech. Eng. Advanced Tech. for Indus. Prod. MEATIPI, Assiut University, pp. 25-33.
- Kyogoku, H., Sugibayashi, T., Ikegami, K, 1987. Strength Evaluation of Scarf Joints Bonded with Adhesive Resin. JSME 30(265), pp. 1052-1059.
- Milašienė, D., Jankauskaitė, V., Arcišauskaitė, R., 2003. Prediction of Stress Relaxation in Laminated Leather Layers. Materials Science (MEDŽIAGOTYRA) 9(1), pp. 73-79.
- Miyano, Y., Shimbo, M., Kunio, T., 1982. Viscoelastic Analysis of Residual Stress in Quenched Thermosetting Resin Beams. Experimental Mechanics 22 (3), pp. 310-316.
- Mori, K., Sugibayashi, T., 1992. Deformation and Strength of Stepped-Lap Joints Bonded with Adhesive Resin. J. of Strain Analysis 27, pp. 171-175.
- Nguyen V., Kedward KT, 2001. Non-Linear Modeling of Tubular Adhesive Scarf Joints Laded in Tension. J. Adhesion 76, pp. 265-292.
- Ozel, A., Kadioglu, F., 2002. "Non-Linear Aanalysis of Adhesively Bonded Single Lap Joint in Bending Load," 10th Int. Conference on Machine Design and Production, September, Turkey, pp. 279-289.
- Rider, A., 1998. "Surface Properties Influencing the Fracture Toughness of Aluminum-Epoxy Joints," Ph.D. Thesis, University of New South Wales.
- Sato, K., Toda, A., 2004. Modeling of the Peeling Process of Pressure-sensitive Adhesive Tapes with the Combination of Maxwell Elements. J. Phys. Soc. Japan, 73, PP. 2135-2141.
- Tsai, M., Morton, J., 1994. A Note on Peel Stresses in Single-Lap Adhesive Joints. ASME J. of Applied Mechanics 61, pp. 712-715.
- Vaziri, A., Hashemi, N., 2002. Dynamic Response of Tubular Joints with an Annular Void Subjected to a Harmonic Axial Load. Int. J. Adhesion and Adhesives 22, pp. 367-373.
- Wang, S.S., Yau, J.F., 1981. "Interfacial Cracks in Adhesively Bonded Scarf Joints," AIAA 19, pp. 1350-1356.
- Yu, X.X., Crocombe, A.D., Richardson, G., 2001. Material Modeling for Rate-Dependent Adhesives. Int. J. Adhesion and Adhesives 21, pp.197-210.